

Human Brain Microwave Imaging Signal Processing: Frequency Domain (S-parameters) to Time Domain Conversion

Kim Mey Chew, Rubita Sudirman, Nasrul Humaimi Mahmood, Norhudah Seman, Ching Yee Yong

Infocomm Research Alliance, Faculty of Electrical Engineering, Universiti Teknologi Malaysia, Johor, Malaysia

Email: rubita@fke.utm.my

Received 2013

ABSTRACT

The paper presents the microwave signal processing method using MATLAB based on the result of microwave imaging system simulation developed using Computer Simulation Technology (CST). The simulation system contains a transmitting/receiving antenna, human brain and a tumor inside the brain model. The source signal, microwave signal operates from 1 to 10 GHz. The generated scattering parameters (S-parameters) are in frequency domain form. This paper describes in detail regarding the signal conversion from frequency domain to time domain through proposed Inverse Fast Fourier Transform (IFFT) method as well as the noise filtering process. Peaks detection process was performed in order to identify the time delay of the reflection points at different Y-axis positions.

Keywords: Microwave Signal; Signal Processing; Scattering Parameters; Time Domain; IFFT

1. Introduction

Since years, lots of microwave engineers put efforts to implement non-ionizing electromagnetic waves in medical field to detect cancer in the human body. The efforts aim to add another alternative for cancer detection besides X-ray and Magnetic Resonance Imaging (MRI).

In return, there is significant progress in using microwaves for breast cancer detection. Microwave imaging enables seeing of the internal structure for an object through the illuminating of the object with low power electromagnetic wave at microwave frequencies. Based on the achievement so far on breast cancer detection research, this study is performed for deeper investigation.

This is a radar-based microwave imaging research where a short pulse is transmitted from a single ultra-wideband (UWB) antenna into the human brain phantom. The back-scattering parameters are detected by the same antenna. This process is repeated for different locations around the human brain phantom. The presence of a tumor would produce strong scattering, and such a response can be interpreted to estimate the location of the tumor. The travel times of signals at various locations are recorded and computed [1].

2. Literature Review

2.1. Scattering Parameters

Microwave imaging is conducted by transmitting a

sequence of electromagnetic waves through the human brain phantom and measuring the scattered field at the perimeter of the phantom. The electromagnetic signals fed to the transmitting antennas and captured by the receiving antennas are characterized by scattering parameters (S-parameters) at the terminal planes to which the two-port vector network analyzer (VNA) is calibrated [2].

The S-parameters measured by the VNA are: S_{nm} and S_{mn} . S_{nn} refers to the ratio of reflected signal at port n to the incident signal at port n while S_{nm} refers to the ratio of transmitted signal measured at port n to the incident signal at port m . Normally, S_{nn} is known as the reflection coefficient at port n and S_{nm} is the transmission coefficient from port m to n .

S_{11} is known as reflection coefficient at antenna 1 under the condition where antenna 2 is terminated in the impedance of its connecting cable at 50Ω to avoid signal enters the region from antenna 2. With the same condition for antenna 2, S_{21} is the forward transmission coefficient of signals from antenna 1 to antenna 2. S_{22} is the reflection coefficient at antenna 2, under the condition that antenna 1 is terminated in the impedance of its connecting cable at 50Ω to avoid signal enters the region from antenna 1. With the same condition for antenna 1, S_{12} is the reverse transmission coefficient of signals from antenna 2 to antenna 1. The S-parameters for N antennas are expressed as [3],

$$\begin{aligned}
 E_{1r} &= S_{11} E_{1i} + S_{12} E_{2i} + S_{13} E_{3i} + \dots + S_{1N} E_{Ni} \\
 E_{2r} &= S_{21} E_{1i} + S_{22} E_{2i} + S_{23} E_{3i} + \dots + S_{2N} E_{Ni} \\
 E_{3r} &= S_{31} E_{1i} + S_{32} E_{2i} + S_{33} E_{3i} + \dots + S_{3N} E_{Ni} \\
 E_{Nr} &= S_{N1} E_{1i} + S_{N2} E_{2i} + S_{N3} E_{3i} + \dots + S_{NN} E_{Ni} \quad (1)
 \end{aligned}$$

This study focused on S_{11} using one antenna as both transmitter and receiver.

2.2. Frequency Domain and Time Domain

The frequency domain is the domain of mathematical functions or signals with respect to frequency rather than time in electronics, control systems engineering and statistics fields [4]. The frequency domain graph shows how much of the signal lies within each given frequency band over a range of frequencies. A change of a signal over time is able to be identified from time-domain graph.

In different field, frequency domain and time domain represent different entity. But all given functions or signals can be converted between the time and frequency domains with a pair of same mathematical operators called a transform. For example, the Fourier transform. Fourier transform decomposes a function into the sum of a potentially infinite number of sine wave frequency components. The 'spectrum' of frequency components is the frequency domain representation of the signal. The frequency domain function can be converted back to time function using inverse Fourier transform.

2.3. Inverse Fast Fourier Transform (IFFT)

There are advantages of analyzing transformed time domain data from frequency domain rather than direct measurement of time domain data [5]. These include better signal-to-noise (SNR) ratio due to the narrowband measurements, the possibility of performing error correction by measuring known standards, as well as the freedom from time jitter and zero-level drift [6]. A variation of Inverse Fast Fourier Transform (IFFT) is used to transform the frequency domain to the time domain. These make the user easier to magnify on their range of interest of the data for specific time or distance.

3. Methodologies

Simulation Modeling

The proposed human brain model was developed using Computer Simulation Technology (CST). Characteristics and specifications of the proposed simulation system are mentioned in [7]. **Figure 1** shows the human brain phantom simulation with and without tumor. In the proposed simulation system, the antenna model moves up to 19 steps along the Y-axis with each step differs by 10 mm apart along the Y-axis.

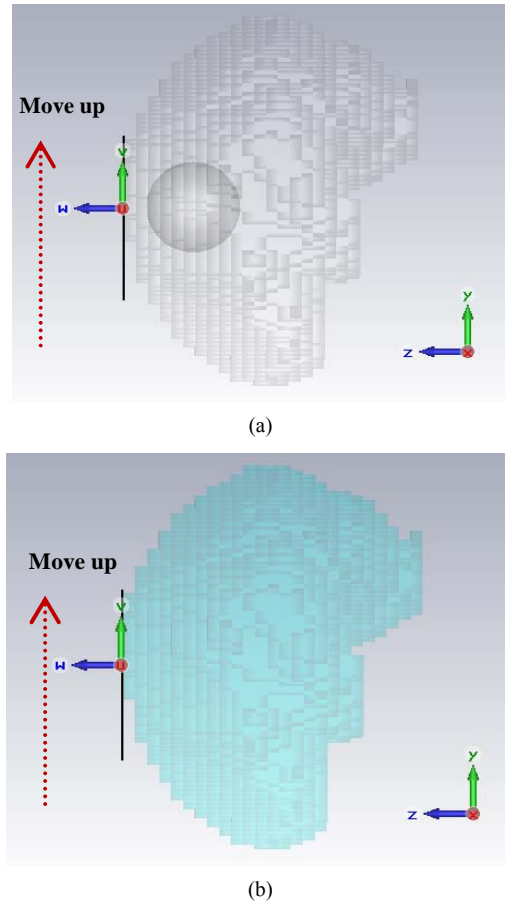


Figure 1. Simulated human brain phantom: (a) With tumor; (b) Without tumor.

4. Result

The S-parameters generated from the simulation system is in frequency domain format, known as frequency domain signal. The main goal of this study is to process the frequency domain signal and transform to time domain format through IFFT method. The transformed time domain results represent the reflection coefficient info for the human brain phantom simulation over time. The signal is then filter to eliminate the noise and ripples.

4.1. Frequency Domain and Time Domain Result

Figure 2 shows the generated frequency domain signal of the human brain phantom simulation with the existence of tumor at 19 different points of microwave penetrating locations along Y-axis. The comparisons for the frequency domain signal of the human brain phantom simulation with and without tumor are described in detail in [7]. **Figure 3(a)** shows the transformation results after IFFT process. Before filter was applied, the signal distorted with ripples. Filter is applied to smooth up the time domain signal for higher accuracy.

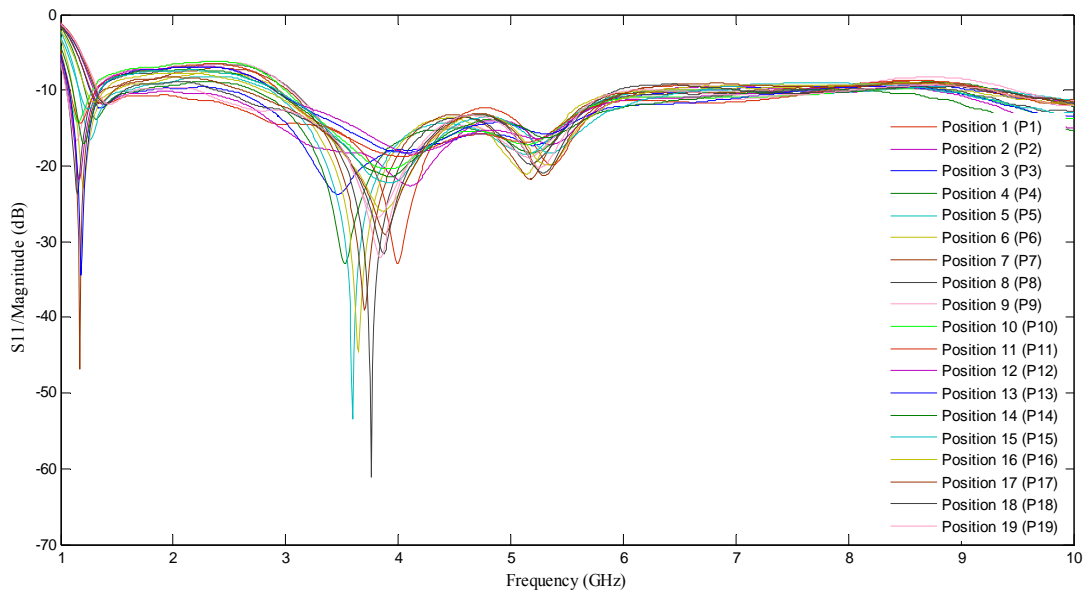
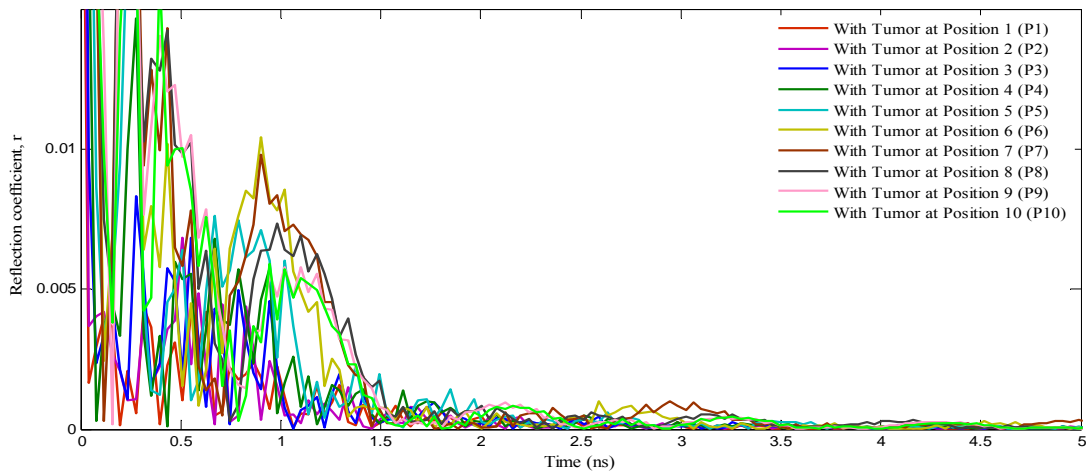
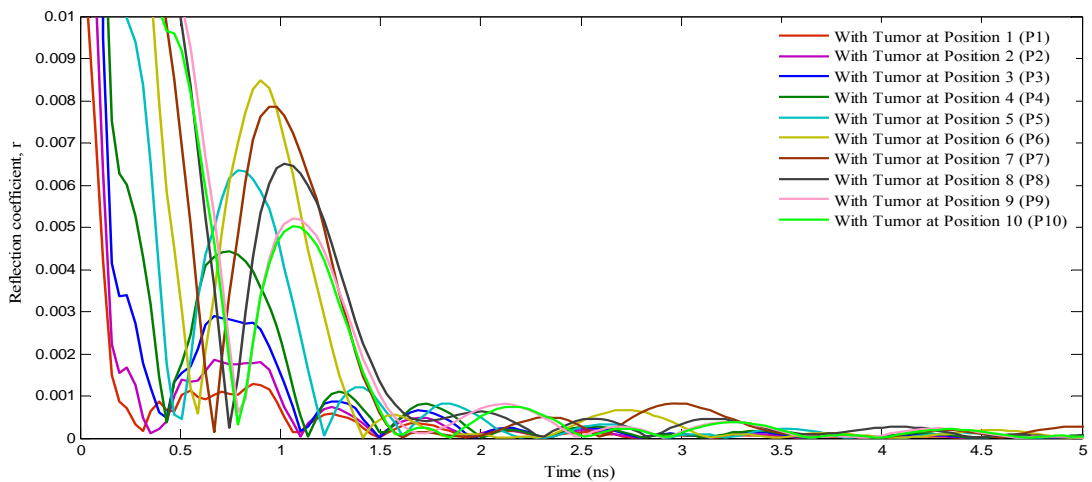


Figure 2. Frequency domain of the simulated human brain phantom contained tumor at 19 different points along Y-axis.



(a)



(b)

Figure 3. Time domain result after IFFT process (a) Without smoothing process; (b) With smoothing process.

4.2. Noise Filtering

A simple MATLAB smoothing method, *mslowess* was applied to filter the time domain result. *mslowess* filter the distorted signal using nonparametric method. *mslowess* assumes the input vector may not have uniformly spaced separation units and therefore, the sliding window for smoothing is centered using the closest samples in terms of the input value but not input index. **Figure 3(b)** shows the filtered time domain result after *mslowess* smoothing process and **Figure 4** shows the zoom plot of the smoothed signal over the original signal.

4.3. Time Delay and Peaks Detection

Figure 5 shows the time domain result of the human brain phantom simulation with and without tumor at position 1, 2, 5, 7, 8, 9 and 19.

In **Figure 5(a)**, the reflection time decrease when the antenna is moving up and close to the human brain model at position 5 to 9. Besides, the reflection points of the human brain phantom model with and without tumor also differ. The reflection point of the human brain model with tumor is slightly delayed from the reflection point of the human brain model without tumor. In **Figure 5(b)**, the reflection coefficient increases when the antenna moving close to tumor. The amplitude shows tumor contributes to the reflection coefficient. In **Figure 5(c)**, the reflection coefficients at position 1, 2 and 19 for both with and without tumor model are slightly the same.

Figure 6 shows the enlarged image of the peaks detection for both human brain model with and without tumor at position 8. From the graph, the reflection time for the human brain model with tumor are slower than the human brain model without tumor.

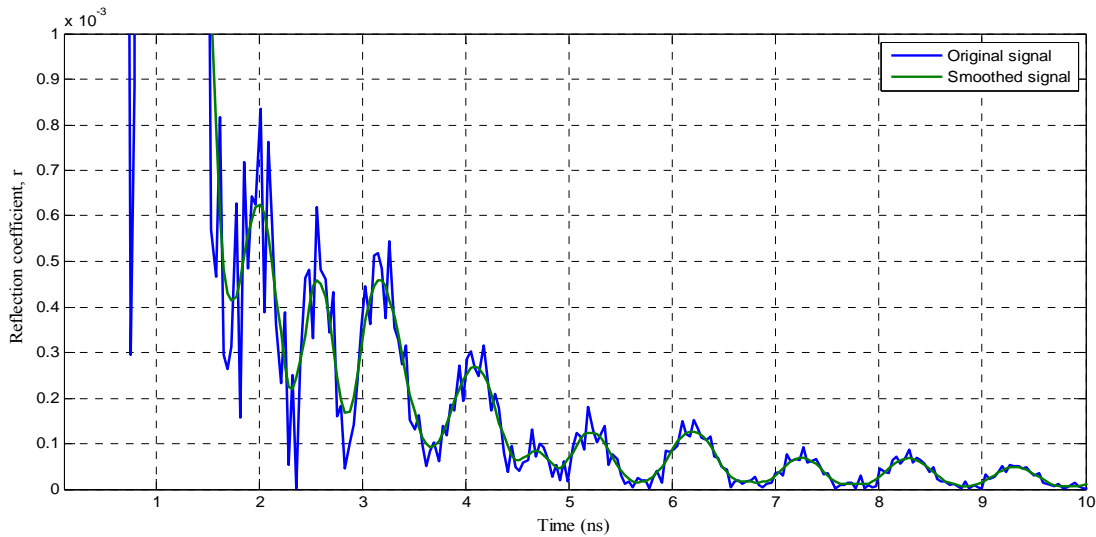
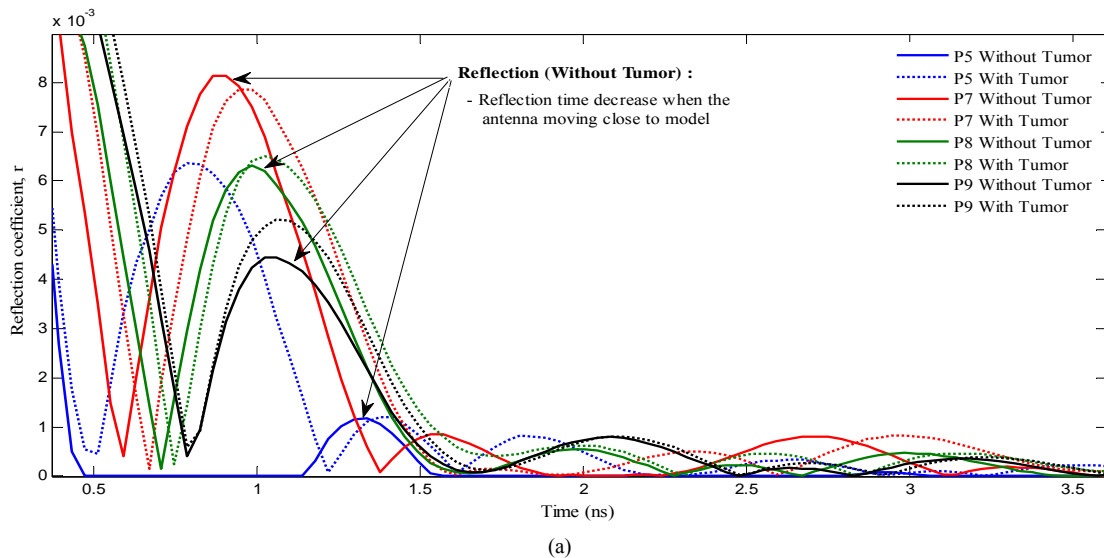


Figure 4. Plot of the smoothed signal over the original signal.



(a)

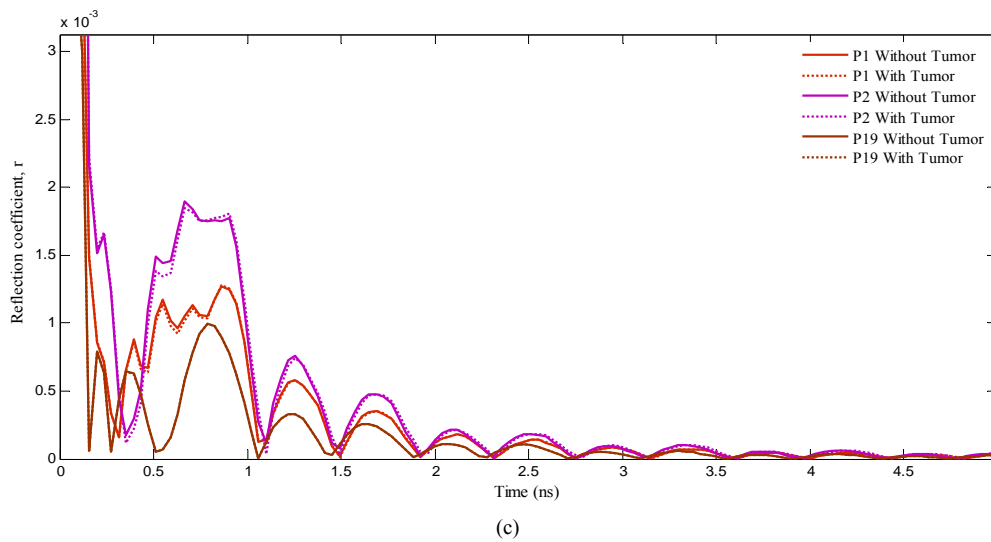
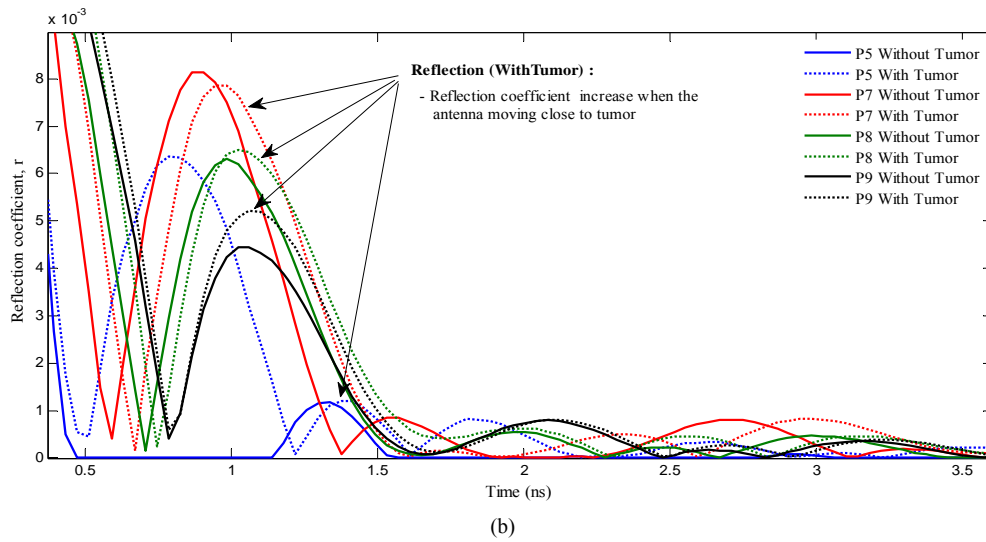


Figure 5. Comparison of time domain result of the simulated human brain phantom with and without tumor.

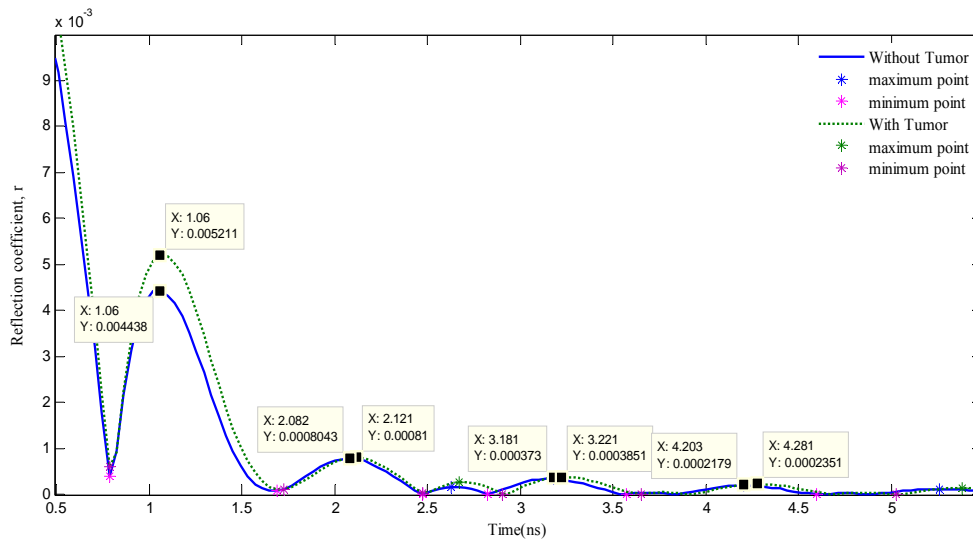


Figure 6. Time domain peaks detection at P8.

5. Discussion

The S-parameters results were generated by the simulation system using the licensed CST software. The simulation system will be enhanced in future by developing more models with different specifications for measurements.

As shown in **Figure 5(a)**, the reflection times were decrease when the antenna is moving up close to the human brain model. This effect was caused by the spherical shape of the human brain model which signals are always reaching to the outer layer of the human brain model at different point of time. The increment of reflection coefficient in **Figure 5(b)** shows both models at the same position were affected by tumor model.

Based on these findings, peaks detection was applied to the transformed time domain signal to mark the reflection points. Image processing was applied to the list of reflection points in order to produce a spatial domain image of the simulation with clearly describing the location of tumor inside the human brain phantom.

6. Conclusions

The obtained S-parameters result was successfully transformed into the time domain format using IFFT method. The *mslowess* smoothing process is filtered up all the noise for a more accurate transformed time domain signal. IFFT was applied to the reflection points of the signal since the time domain signal is appeared easier for visualization and analysis. The reflection points are then processed to produce a spatial domain image of the human brain model with an estimated tumor location. The study is still in a preliminary stage and for future work, different models are developed and processed to enhance the current method in order to develop a human brain tumor detection algorithm.

7. Acknowledgements

The authors are deeply indebted and would like to express our gratitude to the Universiti Teknologi Malaysia for supporting and funding this study under Research Universiti Grant (Q.J130000.2636.05J69). As well as Ministry of Science, Technology and Innovation (MOSTI) grant support (4S056) and MyPhd Scholarship Scheme from Ministry of Higher Education (MOHE). Our appreciation also goes to the Electronics and Bio-medical Instrumentation (bMIE) for their cooperation in the research work.

REFERENCES

- [1] E. C. Fear, "Microwave Imaging of the Breast," *Technology in Cancer Research & Treatment*, Vol. 4, 2005, pp. 69-82.
- [2] G. A. Ybarra, Q. H. Liu, S. P. John and T. J. William, "Chapter 16: Microwave Breast Imaging. Emerging Technology in Breast Imaging and Mammography," American Scientific Publishers, California, USA, 2007.
- [3] W. T. Joines, Q. H. Liu and G. A. Ybarra, "Handbook of Biological Effects of Electromagnetic Fields," CRC Press, Boca Raton, FL, 2005.
- [4] S. A. Broughton and K. Bryan, "Discrete Fourier Analysis and Wavelets: Applications to Signal and Image Processing," New York: Wiley, 2008, p. 72.
- [5] M. E. Hines and H. E. Stinehelfer, "Time-Domain Oscillographic Microwave Network Analysis Using Frequency-Domain Data," *IEEE Trans. Microwave Theory Tech.*, Vol. MTT-22, No. 3, 1974, pp. 276-282.
- [6] Ulriksson and Bengt, "Conversion of frequency-domain data to the time domain," *Proceedings of the IEEE*, Vol. 74, No. 1, 1986, pp. 74-77.
- [7] K.-M. Chew, R. Sudirman, N. H. Mahmood, N. Seman and C.-Y. Yong, "Human Brain Microwave Imaging Simulation System Using Computer Simulation Technology (CST)," *ICIPT2013: 2013 8th International Conference On Information Processing, Management and Intelligent Information Technology (ICIPM, ICIP)*, In press.